Radiolabeled Nanoparticles as Dual-Modality Imaging Agents

Penelope Bouziotis

Director of Research
Radiochemical Studies Laboratory
Institute of Nuclear & Radiological Sciences & Technology, Energy & Safety
National Center for Scientific Research "Demokritos"
Athens, Greece

Nanomedicine: The present and future in personalized therapy,
5th Hellenic Forum for Science, Technology & Innovation
5-7 July 2017, Athens, Greece

Cancer is a broad group of various diseases, all involving unregulated cell growth. In cancer, cells divide and grow uncontrollably, forming malignant tumors, and invade parts of the body.

In 2012 approximately 14 million cancers were diagnosed and 8.2 million people died of cancer worldwide.

Medical tests for suspected cancer patients

- Blood tests

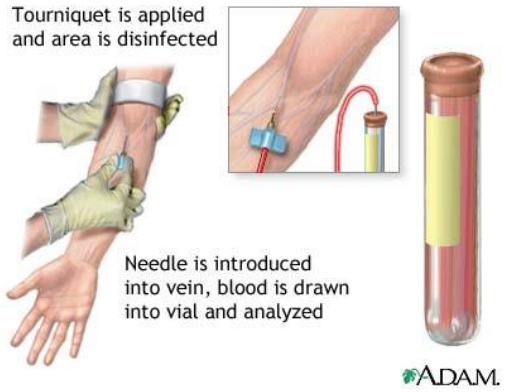

- Endoscopy

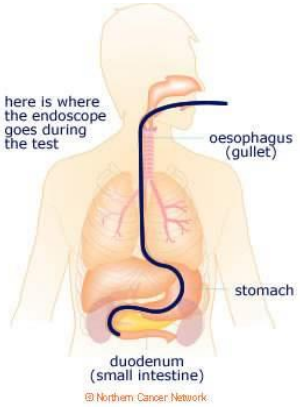

- Imaging techniques

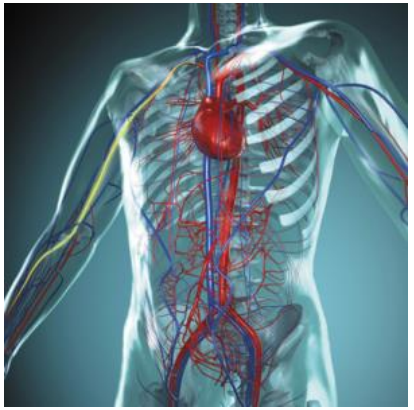

Imaging Techniques

Non ionizing radiation

- Optical Imaging

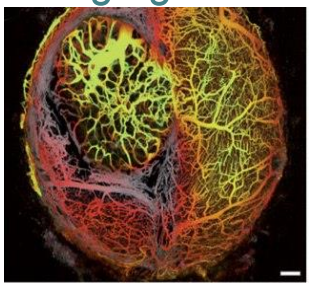

- UltraSonography

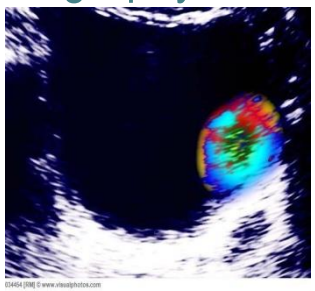

- Magnetic Resonance Imaging (MRI)

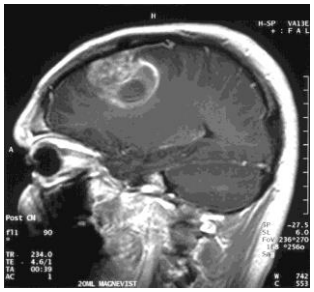

Ionizing radiation

- Radiography

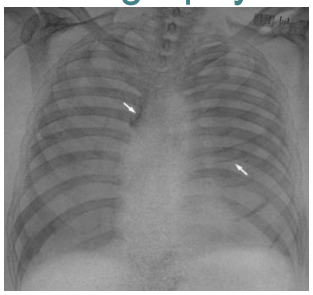

- Computed Tomography (CT)

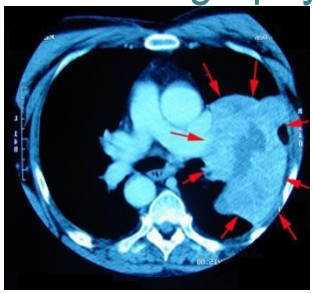

- Nuclear Medicine Techniques (PET and SPECT)

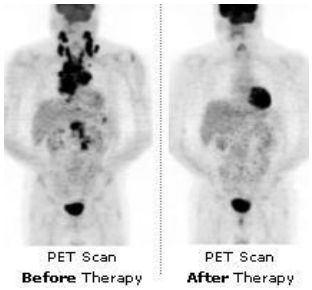

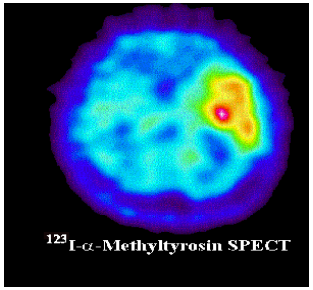

Multimodality Imaging Techniques

No single imaging technique is perfect…

- SPECT/CT
- PET/CT
- SPECT/optical
- PET/optical
- CT/optical
- MRI/optical
- SPECT/MRI
- PET/MRI

PET/CT imaging of bone cancer with hot spots on the ribs and spine

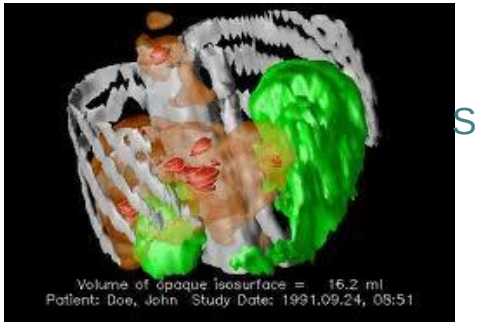

SPECT/CT imaging of liver cancer with hot spots on the liver

The combination of two or more imaging techniques can therefore offer synergistic advantages over any modality alone.

Dual modality PET/MRI or SPECT/MRI probes would provide us images which combine the high spatial resolution of MRI with the high sensitivity of NMT

Hybrid PET/MR Systems

Simultaneous PET/MR scanners

Sequential PET/MR scanners

PET and MRI are largely complementary techniques and the combination would certainly be a ‘marriage of convenience’ – with PET (exceptionally sensitive but with poor spatial resolution) synergistically linked to MRI (giving supremely high-resolution anatomical information in the submillimetre range).

Nanomedicine: The present and future in personalized therapy,
5th Hellenic Forum for Science, Technology & Innovation
5-7 July 2017, Athens, Greece

Nanoparticles as dual-modality imaging agents

The development of hybrid SPECT/MRI and PET/MRI systems has triggered an unprecedented quest for novel dual-modality imaging agents for application to such systems. It is interesting to note that few SPECT/MRI or PET/MRI agents have been reported but, now, with the development of suitable equipment, there is huge scope for the development of hybrid SPECT/MRI and PET/MRI probes.

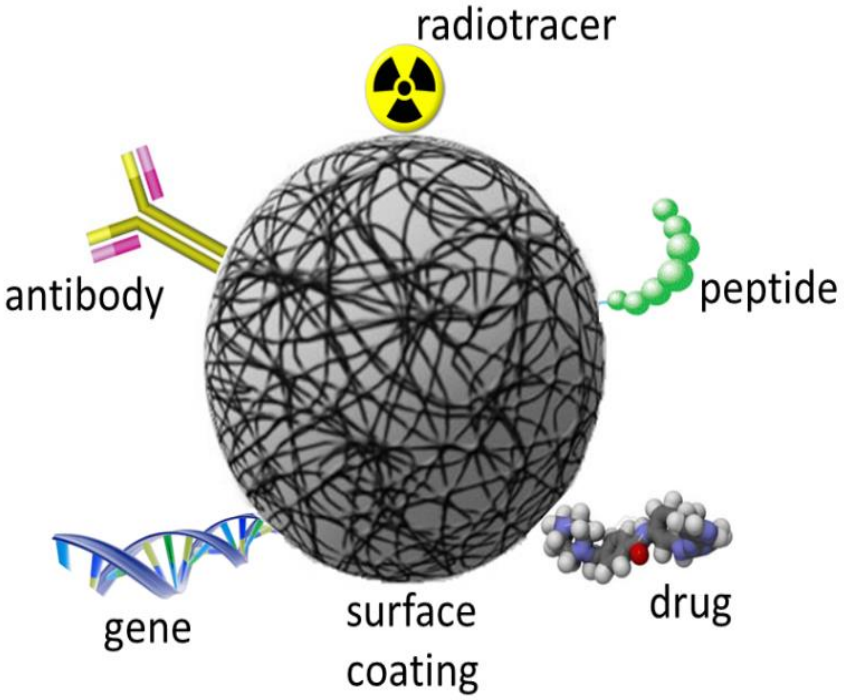

Surface functionalization of nanoparticles allows them to "behave" as dual-modality imaging agents both for SPECT/MRI and PET/MRI applications

Commonly-used Radioisotopes for Nanoparticle Radiolabeling

Radionuclide	$t_{1/2}$(h)	Emission type (%)	Energy (keV)	Mode of Generation	Radiolabeling Methods
^{99m}Tc	6.02	γ, IT	140	^{99}Mo/^{99m}Tc generator	Coordination Chemistry
^{111}In	67.2	Auger e^-, EC	172,247	Cyclotron	Coordination Chemistry
^{67}Ga	78.1	γ, EC	93,185,300	Cyclotron	Coordination Chemistry
^{18}F	1.83	β^+(97), EC (3)	635	Cyclotron	Direct (Nucleophilic or Electrophilic) or Indirect (prosthetic) Labeling
^{64}Cu	12.9	β^+(19.3), β^- (39.6), EC (45)	573,654	Cyclotron	Coordination Chemistry
^{68}Ga	1.14	β^+(90), EC (10)	770,1880	^{68}Ge/^{68}Ga generator	Coordination Chemistry
^{124}I	76.8	β^+(25), EC (75)	790,1530,2130	Cyclotron	Nucleophilic Halogen Exchange Chemistry

Nanoparticle Radiolabeling

Radiolabeling of nanoparticles with metallic radionuclides

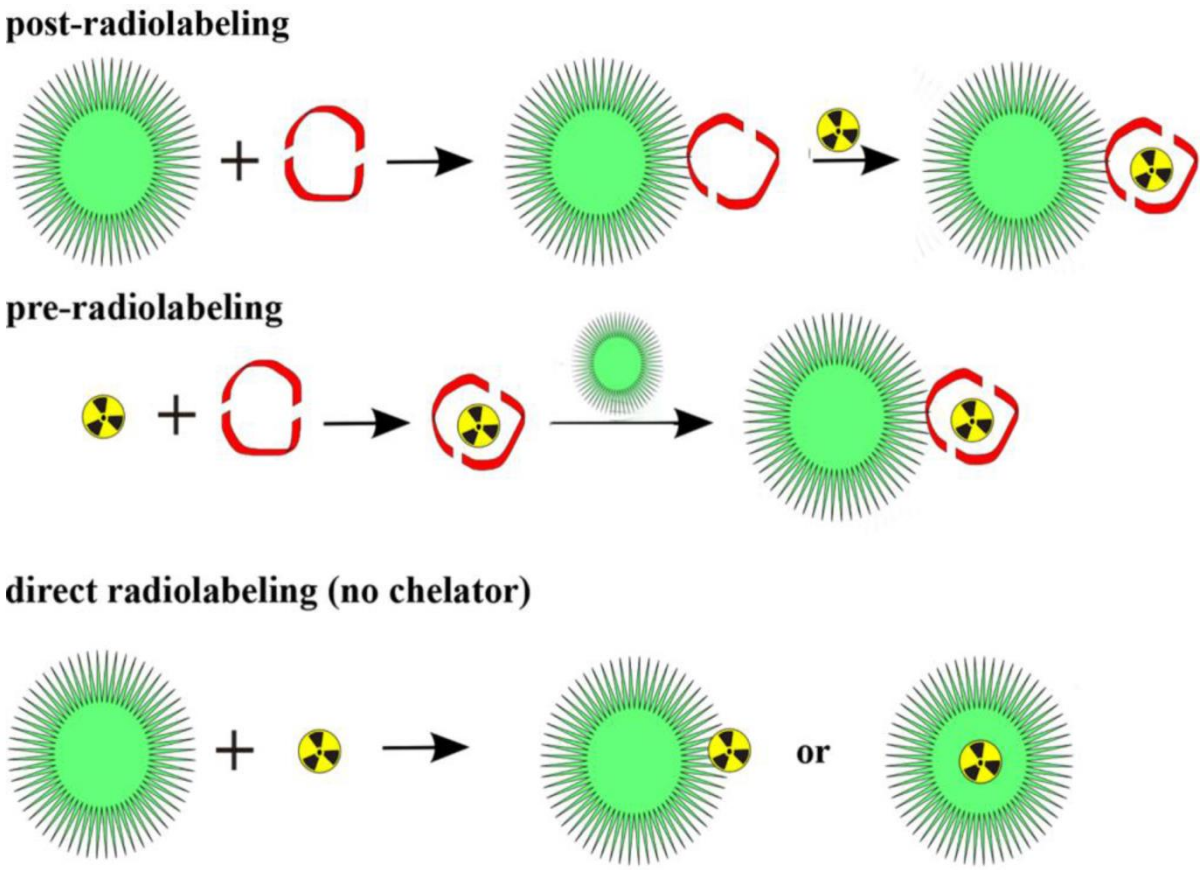

T.L.Ross et al, Radiolabeling of nanoparticles and polymers for PET imaging, Pharmaceuticals 2014; 7(4): 392-418

Nanoparticles as dual-modality PET/MRI imaging probes

A. Schematic diagram of an integrin $a_v b_3$-targeting ^{64}Cu-DOTA-IO-RGD PET/MRI dual-modality probe

B. *A two-dimensional projection* micro-PET image of a mouse bearing an integrin $a_v b_3$-positive U87MG tumor at 4 hours post-injection of the probe.

C. T2-weighted MRIs of mice before and

D. 4 hours after intravenous injection of the probe.

The arrow indicates the tumor

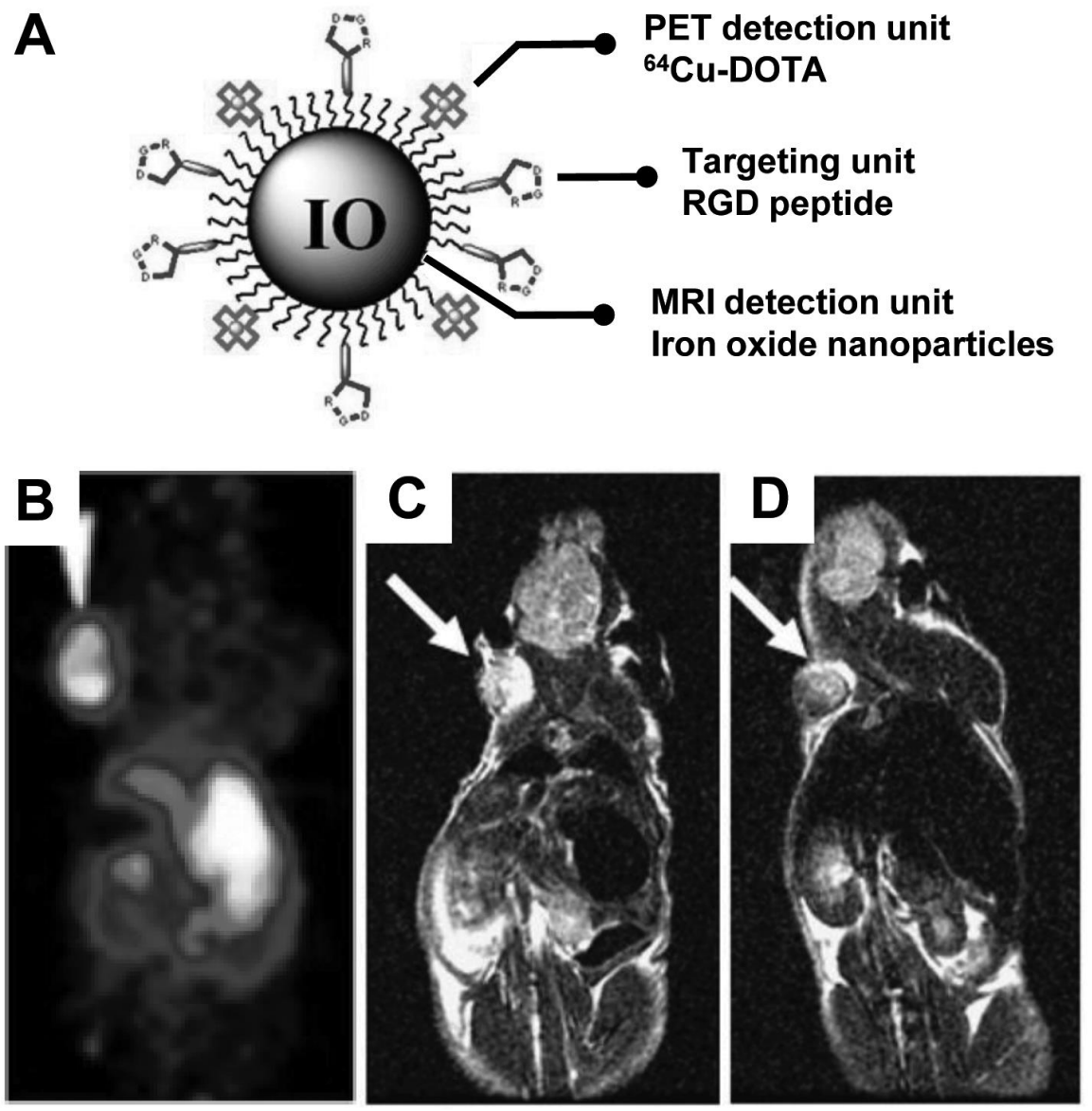

Lee HY, Li Z, Chen K, et al. PET/MRI dual-modality tumor imaging using arginine-glycine-aspartic (RGD)-conjugated radiolabeled iron oxide nanoparticles. J Nucl Med 2008;49:1371–9

Nanoparticles as dual-modality PET/MRI imaging probes

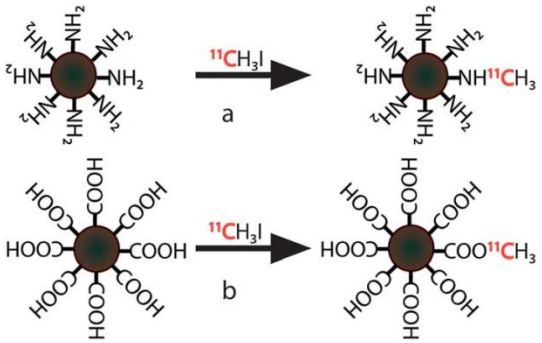

Simultaneous PET/MR images of the ^{11}C-labeled SPIO NPs in a mouse using a 9.4 T MRI small animal scanner.

❖Top row: MRI images show loss of signal from the accumulation of SPIO NPs in the liver.

❖ Middle row: PET images which result from C-11 positron decay show the accumulation of ^{11}C-labeled SPIO NPs in the liver.

❖ Bottom row: Fused PET/MR images show the exact correspondence of the two signals.

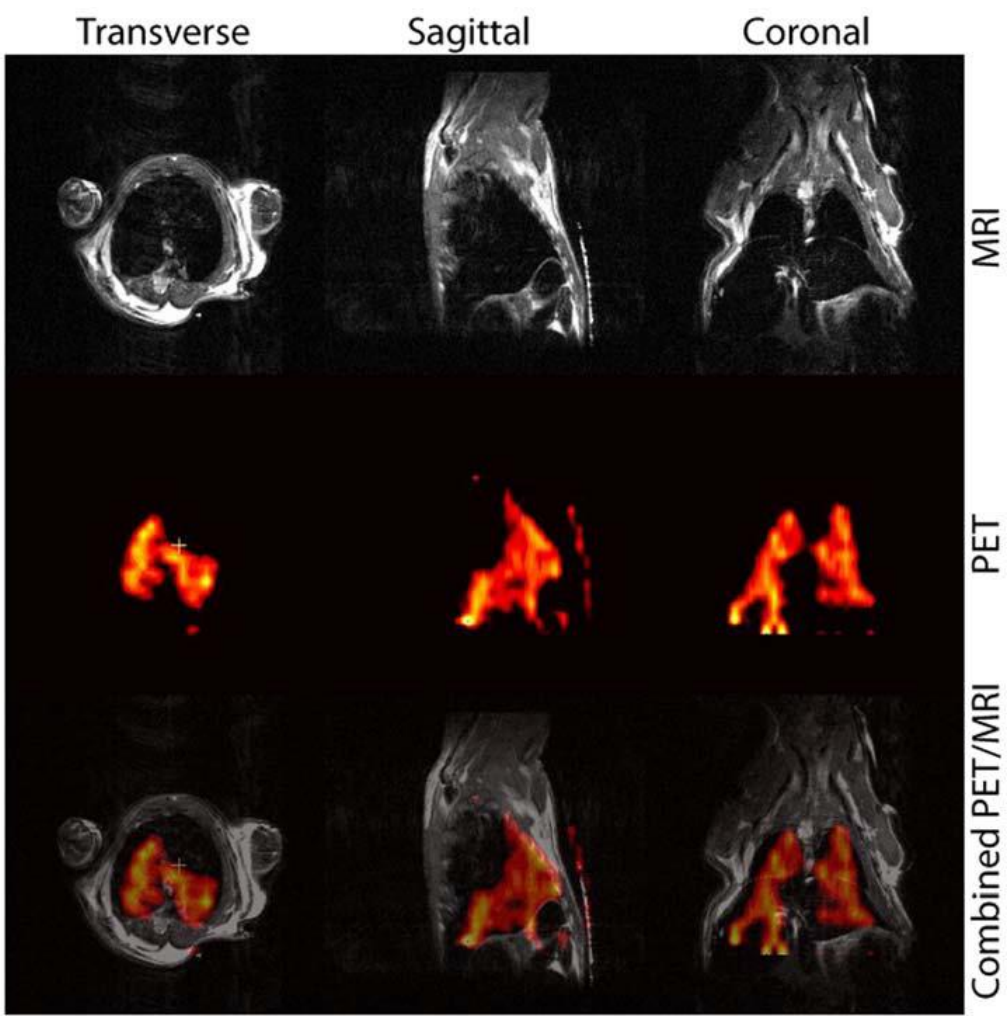

Sharma R. et al, "Carbon-11 radiolabeling of iron-oxide nanoparticles for dual-modality PET/MR imaging", Nanoscale, 2013, 5, 7476

Nanoparticles as dual-modality PET/MRI imaging probes

Chelator-free radiolabeling of iron oxide nanoparticles with a silica shell.
In vivo mouse images of:

(a) 10 MBq/50 μg Fe of ^{68}Ga labeled iron oxide nanorods, fused PET-CT coronal slice image showing areas of main organ uptake at 80–90 minutes post-injection
(b) 10 MBq/50 μg Fe, T_2 weighted MR image at 90 minutes post-injection
(c) control mouse without nanoparticle administration, T2 weighted MR image at 90 minutes post-injection
(d) time-activity-curve for major organs from PET image after administration of 10 MBq/50 μg Fe.

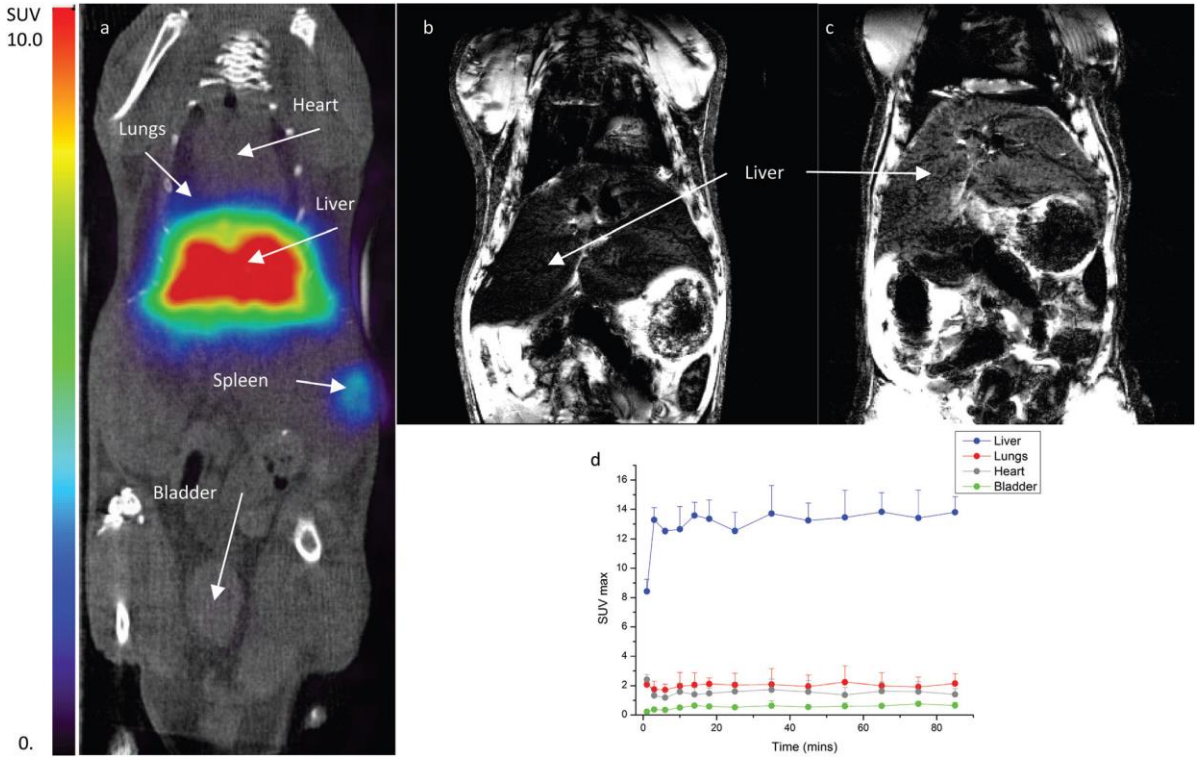

Burke, B. P. et al 2015. "Chelator free gallium-68 radiolabelling of silica coated iron oxide nanorods via surface interactions", Nanoscale, 2015, 7, 14889-14896.

Nanoparticles as dual-modality SPECT/MRI imaging probes

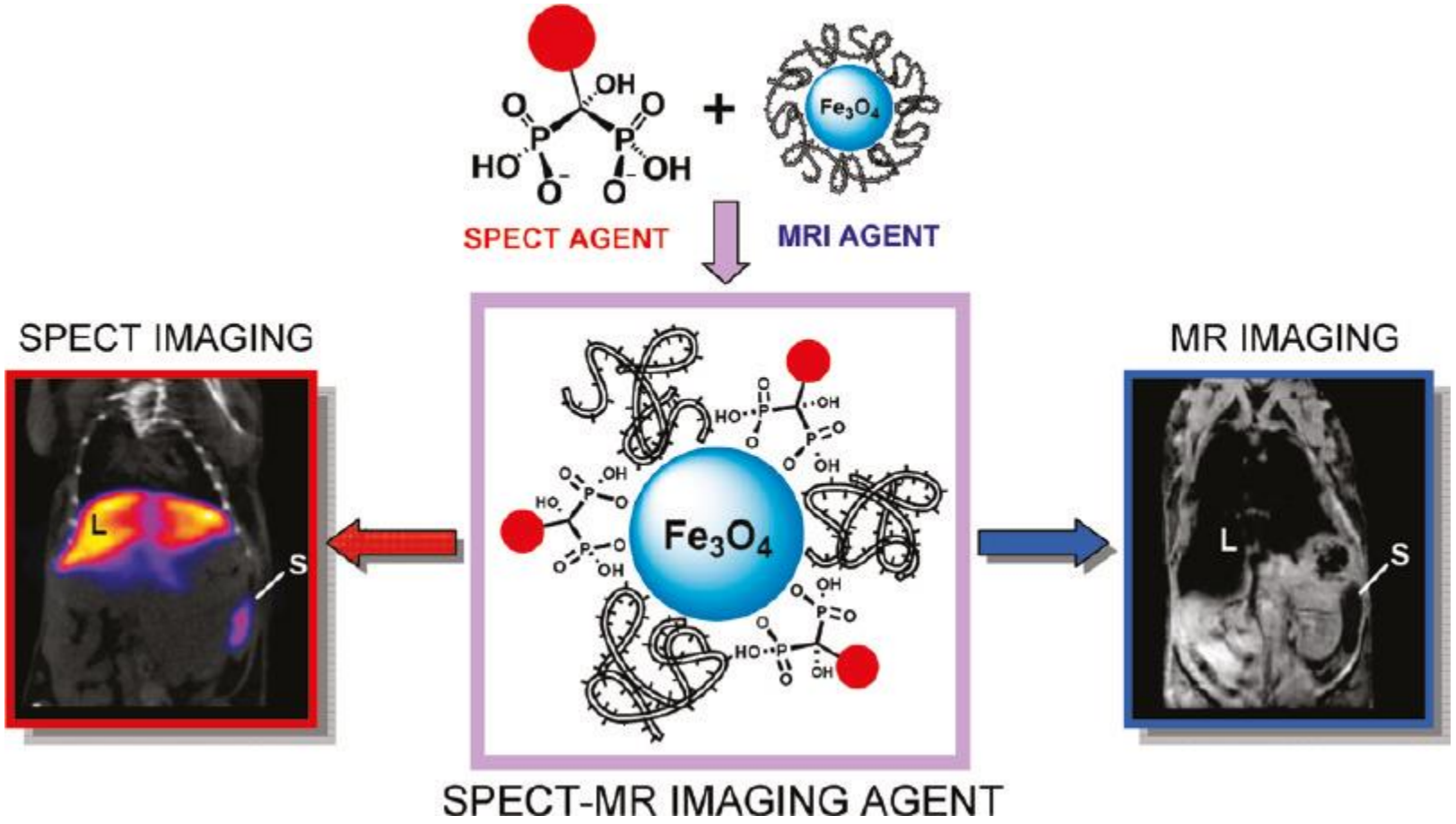

Rafael T. M. de Rosales et al, ^{99m}Tc-Bisphosphonate-Iron Oxide Nanoparticle Conjugates for Dual-Modality Biomedical Imaging, Bioconjugate Chemistry 2011; 2: 455-465

Bevacizumab-conjugated SPIONs

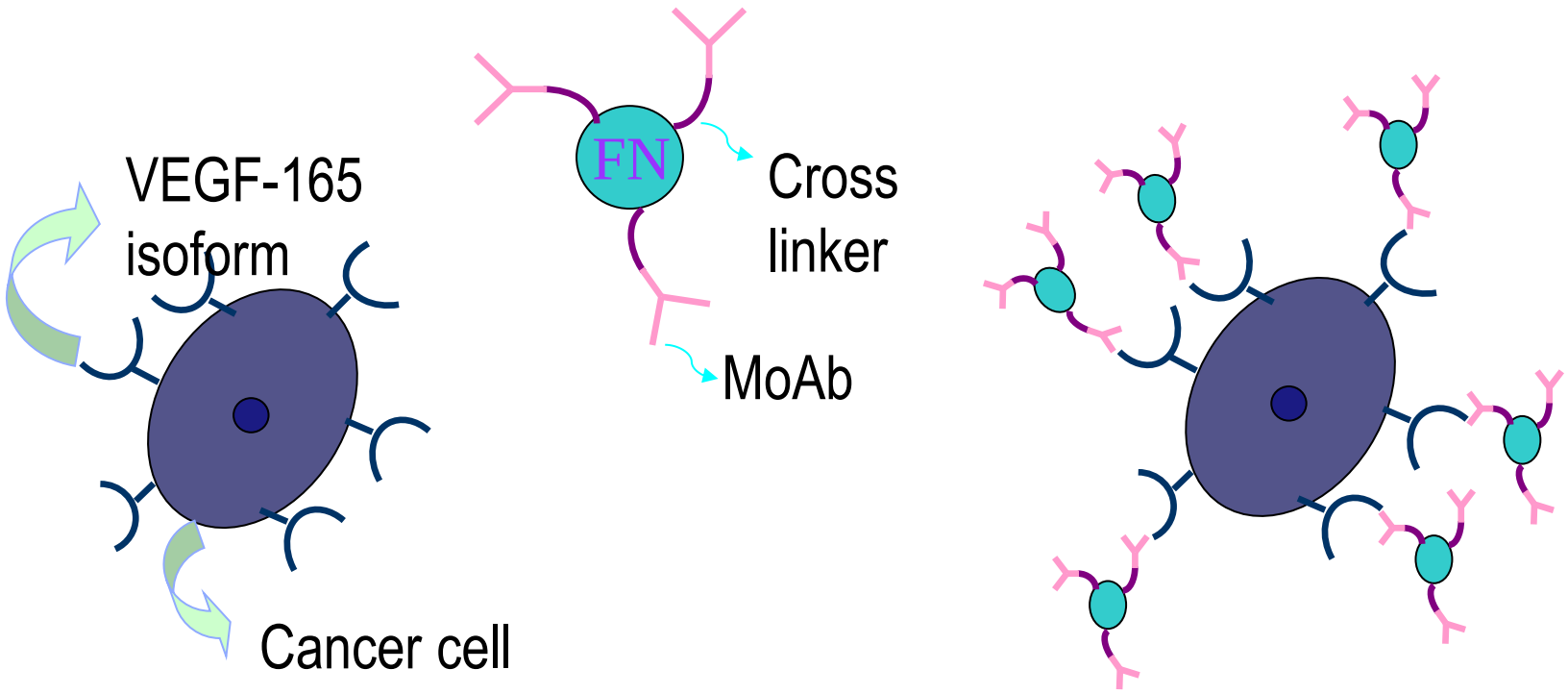

Schematic representation of bevacizumab-conjugated ferromagnetic nanoparticles (Bc-FNs) and their binding to M165 cancer cells overexpressing the VEGF-165 isoform.

Binding efficiency of Bevacizumab-conjugated SPIONs

- M165 cells were plated in 6-well plates for 24 h
- Bevacizumab conjugated-FNs were added at predetermined concentrations (1 mM Fe and 5 mM Fe per well)
- After I h incubation at 4 °C, the supernatant was removed and the cells were carefully washed with PBS
- The cells were incubated with goat antihuman IgG-FITC for 2 h, washed using PBS three times, treated with paraformaldehyde (4%, 0.5 mL) for 10 min to fix the cells, and then washed with PBS.
- The cells were visualized with fluorescence microscopy

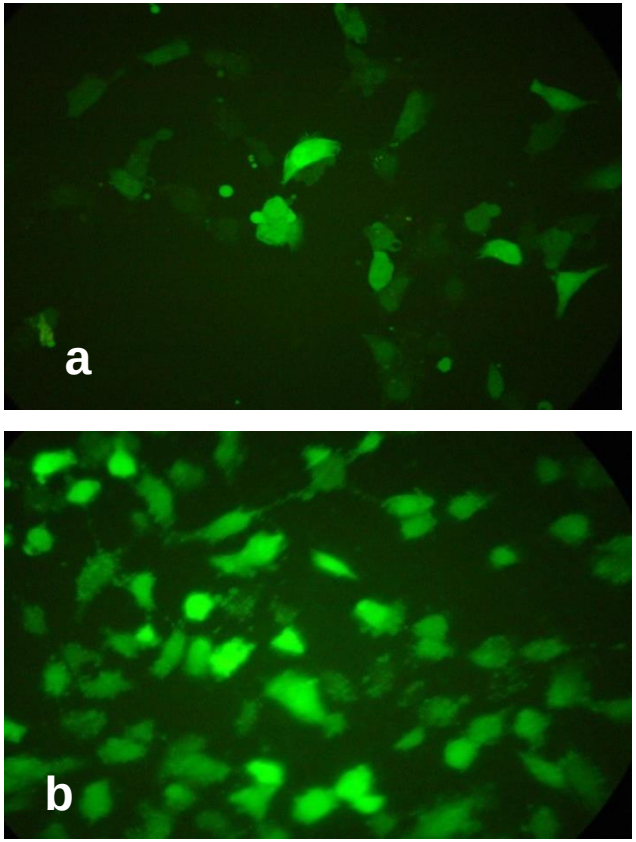

Fluorescence microscopy of Bc-FN bioconjugates incubated with M165 cells overexpressing the VEGF-165 isoform. Vivid green fluorescence indicative of successful VEGF-165 targeting is detected for M165 cells treated with the Bc-FNs (b), as opposed to the same cells treated with a control conjugate (a)

Radiolabeling of Bevacizumab-SPIONs with Technetium-99m: ex vivo and in vivo assessment

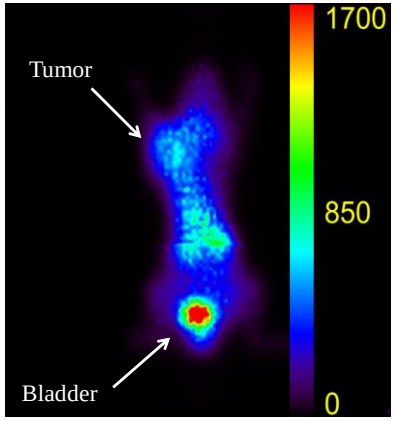

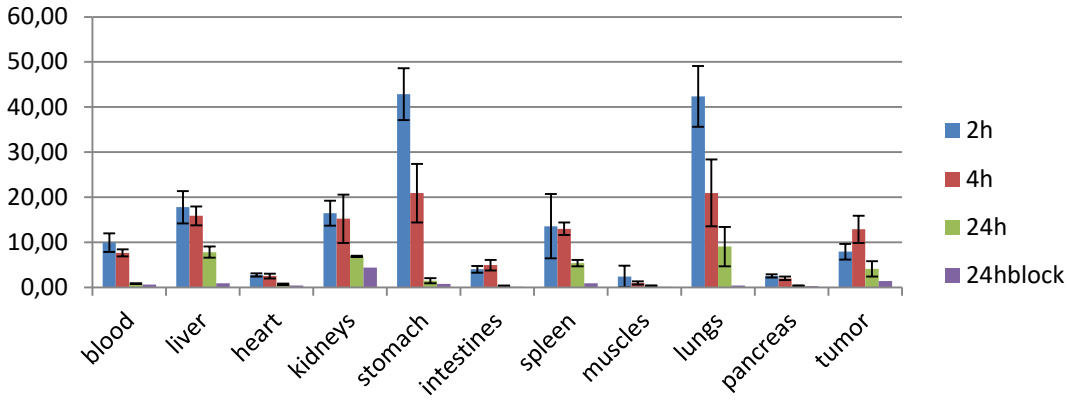

Accumulation of NPs-DMSA-SMCC-bevacizumab-^{99m}Tc in the tumor from 2h p.i. (7.9% ± 2.6%), remaining relatively high even at 24h p.i. (4.1% ± 1,7% ID/g)

Passive accumulation of NPs-DMSA-^{99m}Tc showed minimal tumor uptake (2.1% ± 0.34% ID/g vs 1.9% ± 0.2% ID/g at 2 and 24h, respectively)

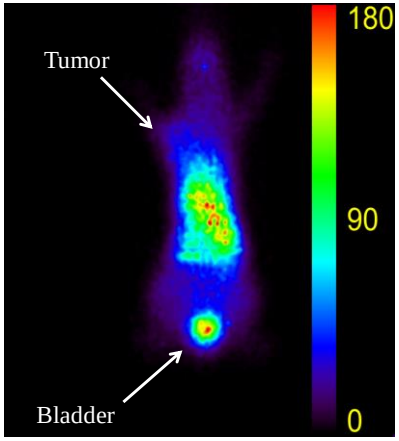

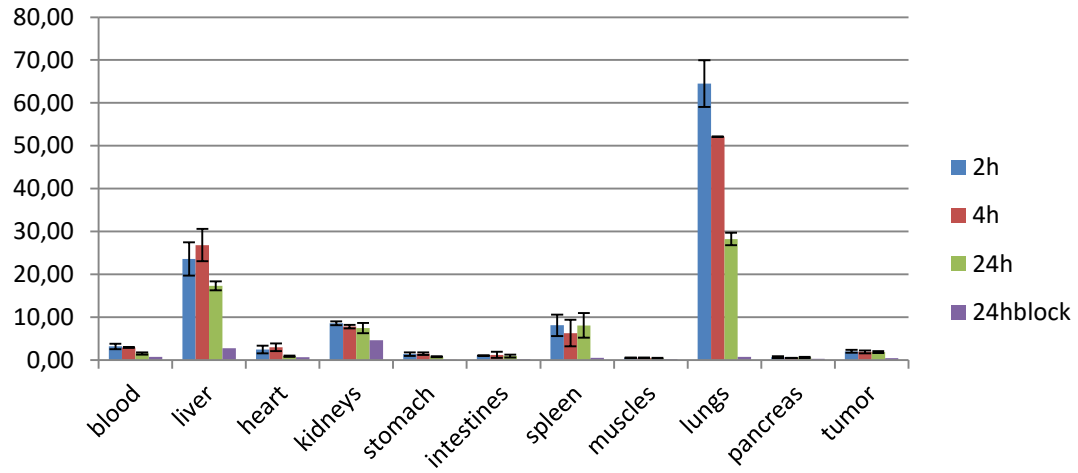

Scintigraphy of NPs-DMSA-SMCC-bevacizumab-^{99m}Tc showed a clear visualization of the tumor, while for NPs-DMSA-^{99m}Tc the tumor could not be visualized.

AGuIX Preclinical Multimodal Probe Theragnostic Nanoparticles MRI-SPECT/PET-Fluorescence-Therapy

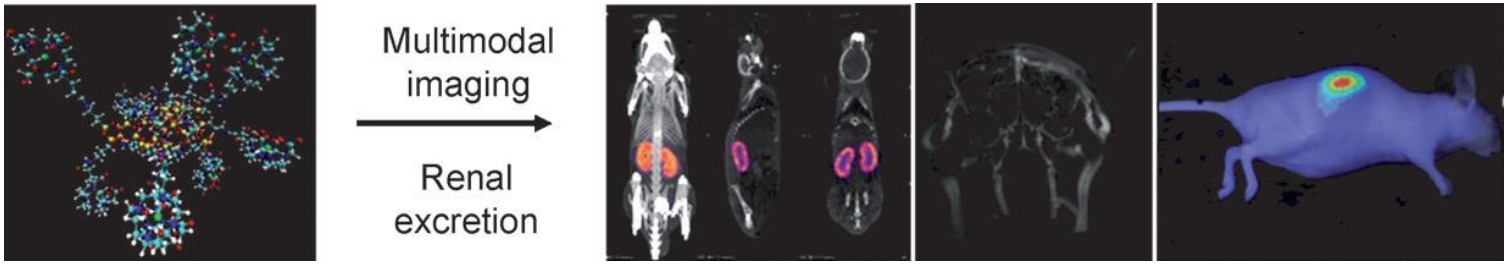

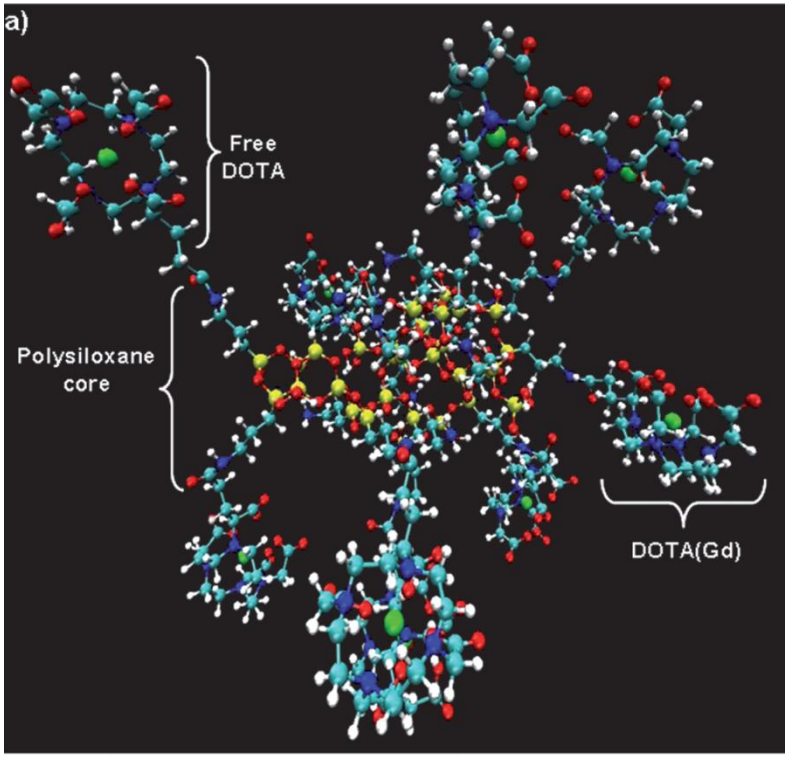

Lux F., et al, "Ultrasmall Rigid Particles as Multimodal Probes for Medical Applications", Angew. Chem. Int. Ed. 2011, 50, 1 – 6

Ultrasmall size
4±1 nm – renal excretion
MW 8.5±2 kDa

Polysiloxane composition
Easy further functionalization

DOTA (Gd) (MRI-Radiotherapy)
FDA approved

Radiometal (M*) chelation
PET/SPECT/Therapy

AGuIX nanoparticles: Ultrasmall particles for Gd-MRI and ^{68}Ga-PET dual-modality imaging

Nanoparticles made of polysiloxane matrix and surrounded by DOTAGA[Gd^{3+}] and NODAGA[$^{68}Ga^{3+}$] have been synthesized for PET/MRI dual imaging. Characterizations were carried out in order to determine the nature of the ligands available for radiolabelling and to quantify them. High radiolabelling purity (>95%) after ^{68}Ga labelling was obtained. MR and PET images demonstrate the possibility to use the nanoparticles for combined PET/MRI scanners. The images show fast renal elimination of the nanoparticles after intravenous injection.

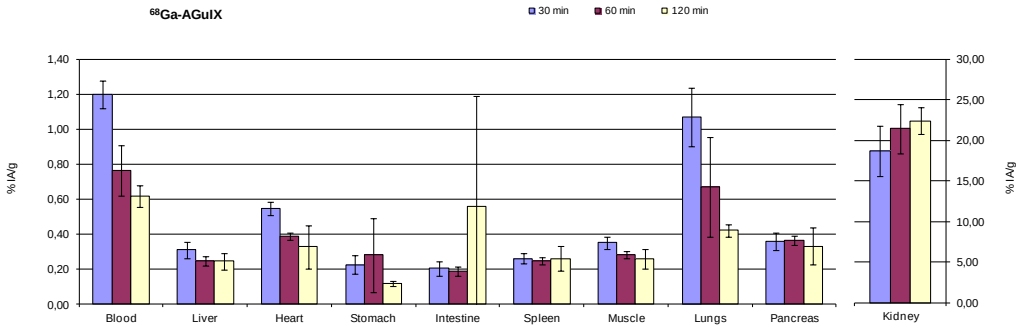

Figure 2: Biodistribution of ^{68}Ga-AGuIX in normal mice at 30, 60 and 120 min p.i.

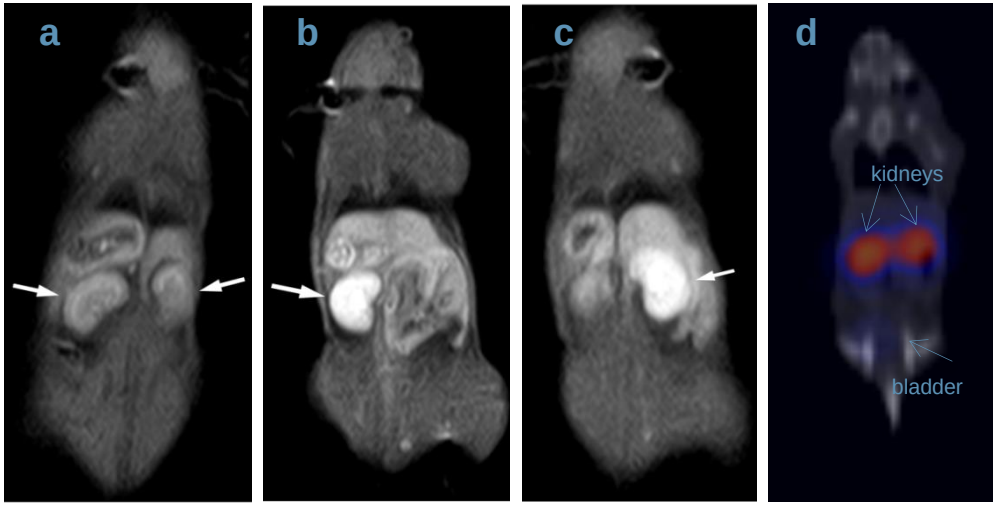

MRI/PET images on the same mouse with AGuIX. MR images of a male mouse (a,b,c), which was injected with Gd-AGuIX, 60 min prior to the MRI exam. We note a definite enhancement of the kidneys (arrows in b and c). Compare with corresponding slices of the kidneys (arrows in a) of a non-injected male mouse, acquired with the same imaging parameters; d) PET/CT image with ^{68}Ga-AGuIX.

C. Truillet, P. Bouziotis, C. Tsoukalas, J. Brugière, M. Martini, L. Sancey, T. Brichart, F. Denat, F. Boschetti, U. Darbost, I. Bonnamour, D. Stellas, C.D.Anagnostopoulos, V. Koutoulidis, L.A. Moulopoulos, P. Perriat, F. Lux and O. Tillement, "Ultrasmall particles for Gd-MRI and ^{68}Ga-PET dual imaging", Contrast Media and Molecular Imaging, 2015

AGuIX nanoparticles:
Ultrasmall particles for Gd-MRI and ^{68}Ga-PET dual-modality imaging

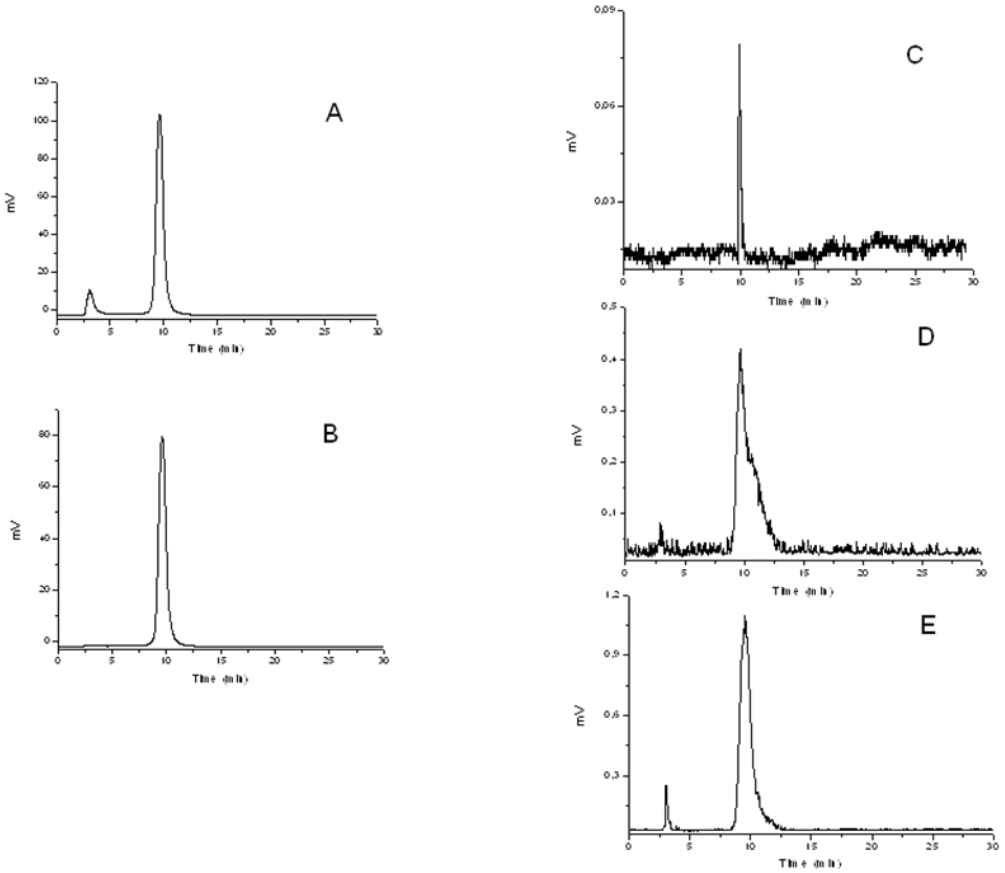

Metabolite studies of ^{68}Ga-AGuIX@NODAGA in tumor (C), blood (D) and urine (E) of tumor-bearing mice, at 60 min post-injection (the pre- and post-purification HPLC curves, (A) and (B) respectively, are given as a reference)

AGuIX nanoparticles:
Ultrasmall particles for Gd-MRI and ^{68}Ga-PET dual-modality imaging

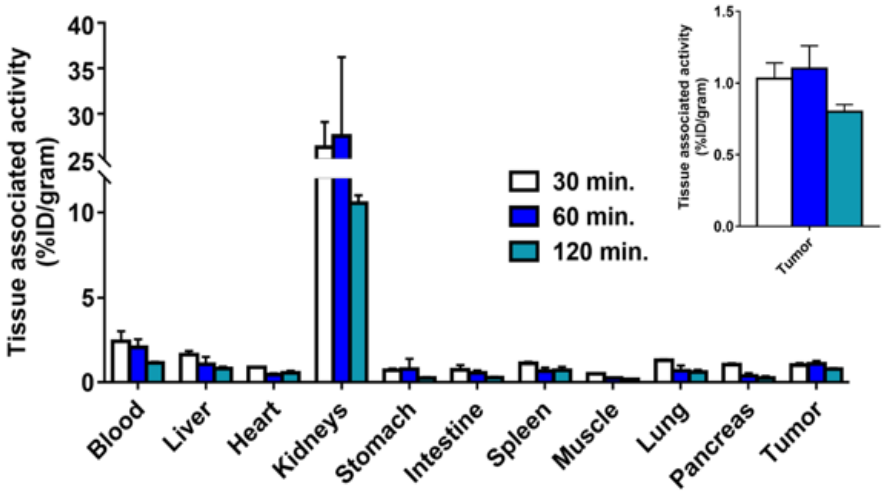

Biodistribution of ^{68}Ga-AGuIX@NODAGA in U87MG tumor-bearing mice

Tumor-to-tissue ratios of ^{68}Ga-AGuIX@NODAGA at 30, 60 and 120 min post-injection

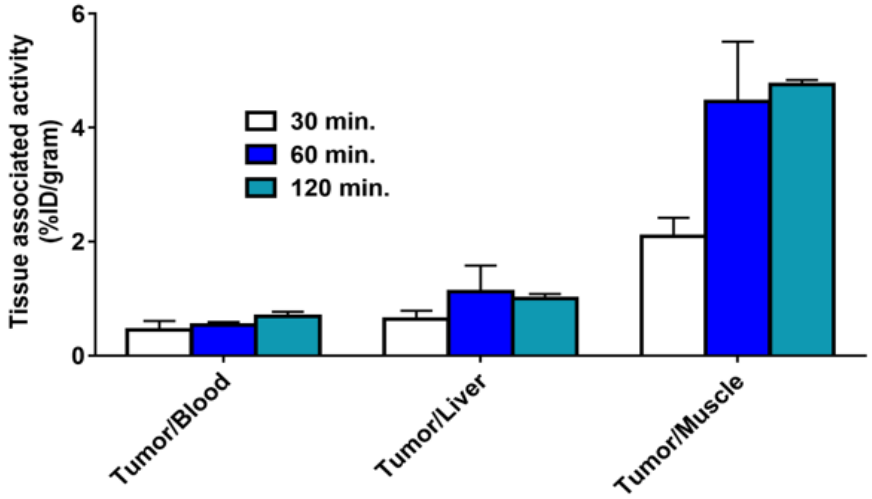

Gd-MRI and ^{68}Ga-PET imaging

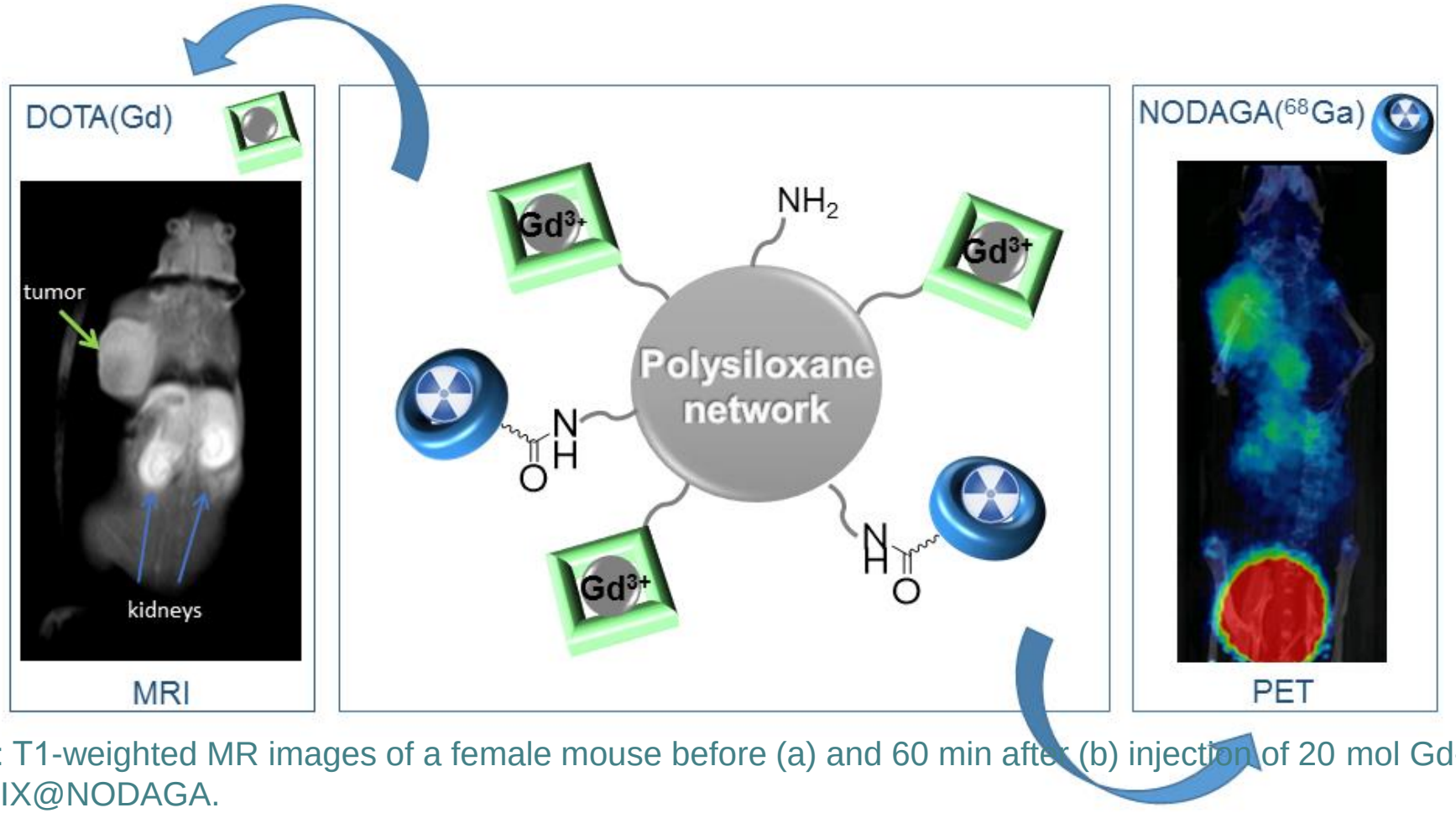

Left: T1-weighted MR images of a female mouse before (a) and 60 min after (b) injection of 20 mol Gd-AGuIX@NODAGA.
Right: PET image of a U87MG tumor-bearing mouse injected with ^{68}Ga-AGuIX@NODAGA, at 60 min p.i.

Bouziotis P, Stellas D., ThomasE., Truillet C., Tsoukalas C., Lux F., Tsotakos T., Xanthopoulos S., Paravatou-Petsotas M., Gaitanis A., Moulopoulos L., Koutoulidis V., Anagnostopoulos C.D., Tillement O., "^{68}Ga-radiolabeled AGuIX nanoparticles as dual-modality imaging agents for PET/MRI guided radiation therapy", Nanomedicine, July 2017

Nanomedicine: The present and future in personalized therapy, 5th Hellenic Forum for Science, Technology & Innovation 5-7 July 2017, Athens, Greece

Histopathological studies

A and B: Gross anatomic features of ^{68}Ga-AGuIX@NODAGA injected mouse post mortem.

C: PET/CT overlay image verifies the accumulation of ^{68}Ga-AGuIX@NODAGA NPs in the tumor. ^{68}Ga-AGuIX@NODAGA NPs are also weakly present in the liver.

D: The gross anatomy of the U87MG generated tumor after the excision.

E and F: Low magnification (scale bar = 200 μm) and high magnification (scale bar = 100 μm) of the U87MG tumor stained with Hematoxylin and Eosin. It is noteworthy that the ^{68}Ga-AGuIX@NODAGA NPs are trapped inside the tumor parenchyma, especially in areas where necrotic features are more evident.

G and H: Higher magnification of the U87MG tumor. With an arrow we indicate the necrotic area and with arrowheads the location of the nanoparticles (scale bar = 25 μm

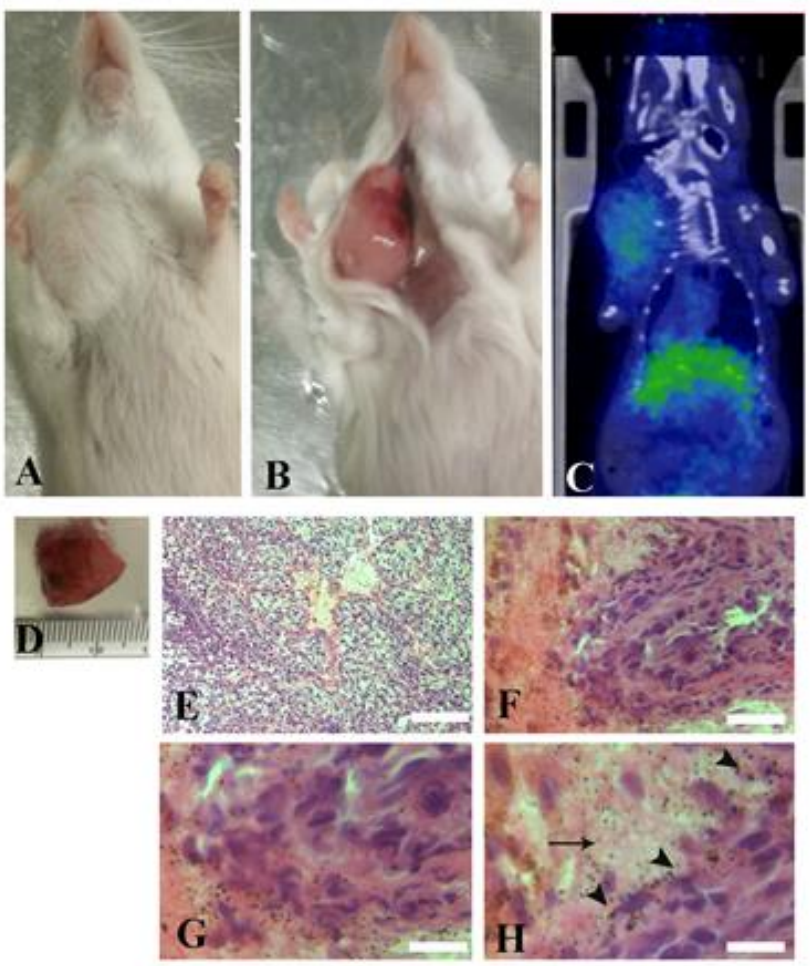

Bouziotis P, Stellas D., ThomasE., Truillet C., Tsoukalas C., Lux F., Tsotakos T., Xanthopoulos S., Paravatou-Petsotas M., Gaitanis A., Moulopoulos L., Koutoulidis V., Anagnostopoulos C.D., Tillement O., "^{68}Ga-radiolabeled AGuIX nanoparticles as dual-modality imaging agents for PET/MRI guided radiation therapy", Nanomedicine, July 2017

AuDTDTPA Gold Nanoparticles

Functionalized gold nanoparticles were applied as contrast agents for both in vivo X-ray and MRI

Synthesis

Encapsulation of gold cores within a multilayered organic shell which is composed of gadolinium chelates bound to each other through disulfide bonds.

MRI contrast enhancement

Due to the presence of Gd ions entrapped in the organic shell

X-ray absorption

Provided by the gold core
Due to the presence of Gd ions entrapped in the organic shell

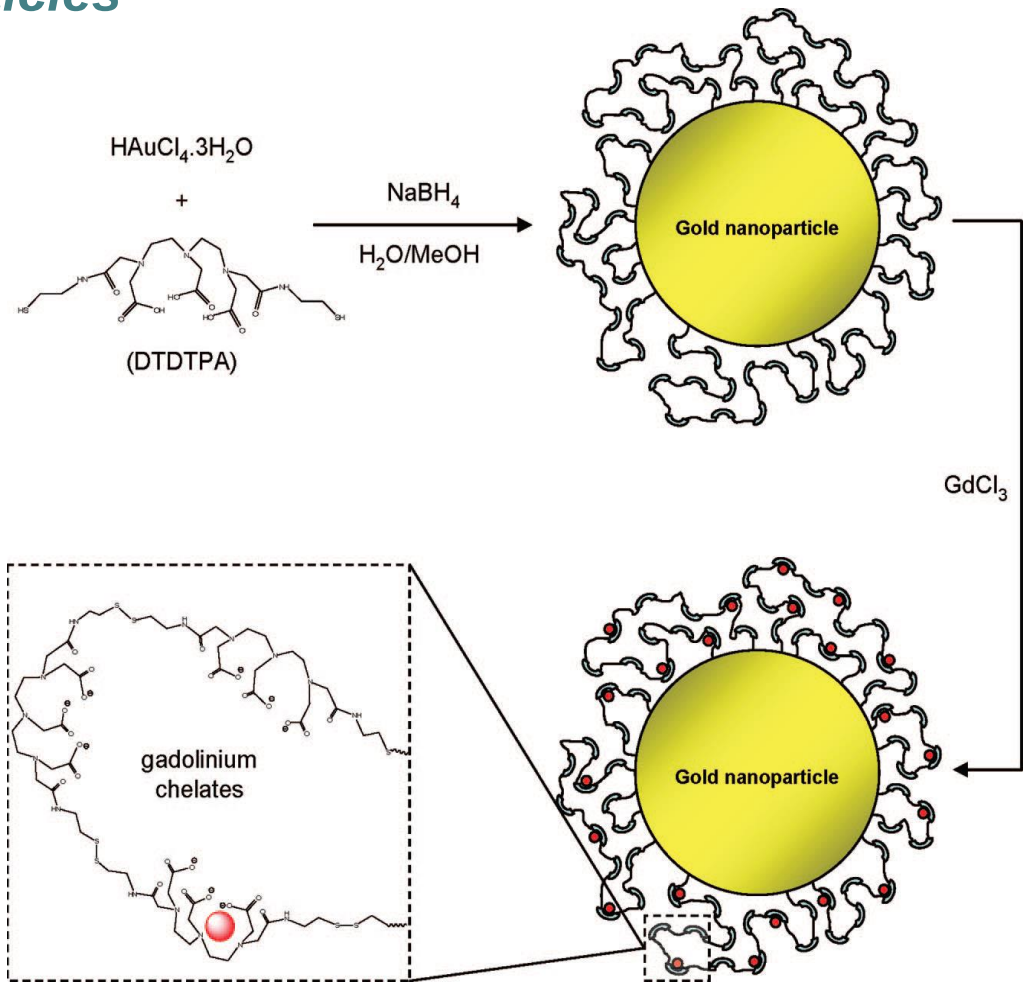

Alric C., et al, "Gadolinium Chelate Coated Gold Nanoparticles As Contrast Agents for Both X-ray Computed Tomography and Magnetic Resonance Imaging", J. AM. CHEM. SOC. 2008, 130, 5908–5915

This study revealed that these particles suited for dual modality imaging freely circulate in the blood vessels without undesirable accumulation in the lungs, spleen, and liver.

AuDTDTPA Gold Nanoparticles

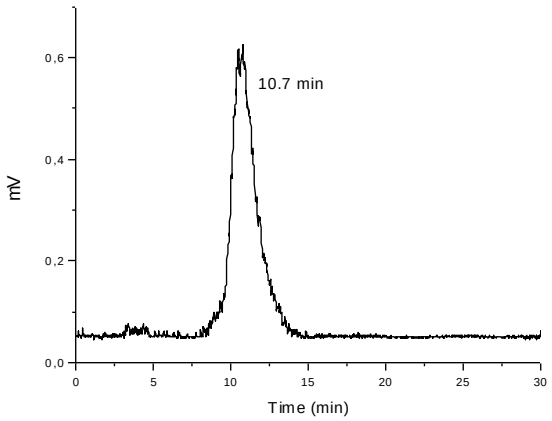

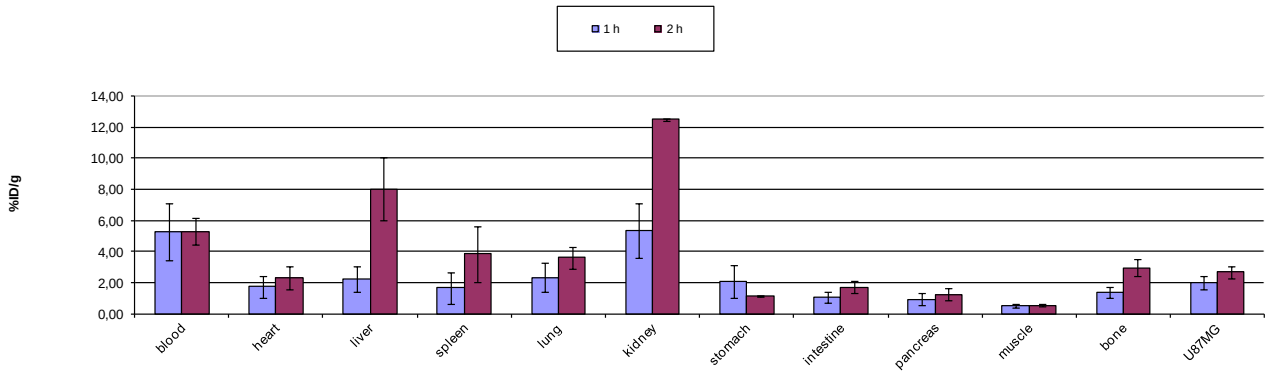

Biodistribution studies for ^{68}Ga-Au@DTDTPA-RGD radiolabeled nanoparticles

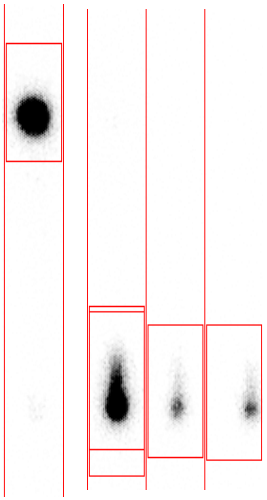

In vitro serum stability study of 68Ga-AGuIX.
From left to right:

^{68}Ga-eluate
^{68}Ga-Au@DTDTPA-cRGD
^{68}Ga-Au@DTDTPA-cRGD/serum stability 20min
^{68}Ga-Au@DTDTPA-cRGD/serum stability 120min

Mobile phase: 0.2M KCL pH 3

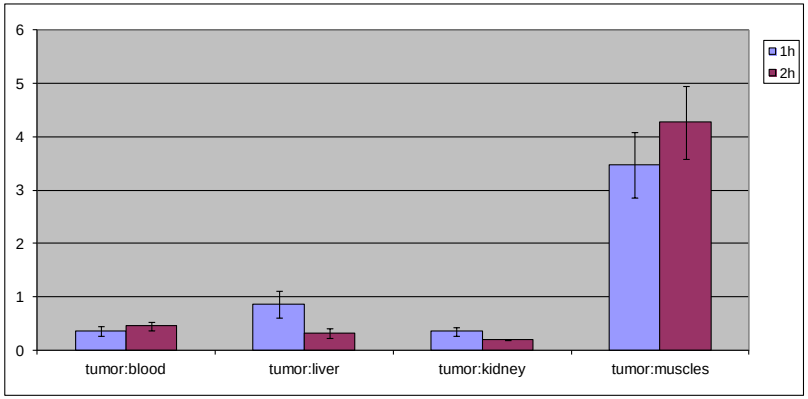

Key tumor-to-tissue ratios of ^{68}Ga-Au@DTDTPA-RGD

In vivo PET imaging studies

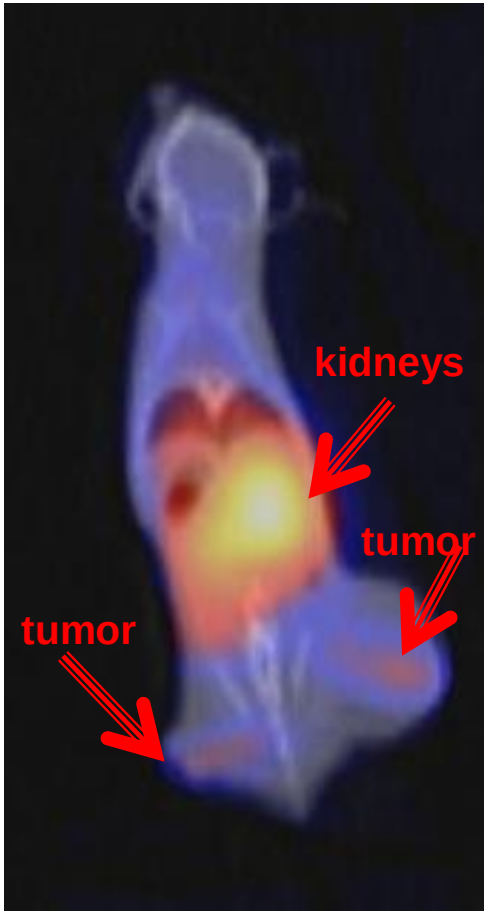

PET/CT imaging of a U87MG tumor-bearing SCID mouse, at 1 h p.i.

The preliminary results of this study warrant the need for further development of Au@DTDTPA-RGD nanoparticles radiolabeled with Ga-68, as a possible dual-modality PET/MRI imaging agent.

Meticulous investigation of the quantities of injected Gd/^{68}Ga-Au@DTDTPA needs to be performed, in order to achieve the optimum tracer concentration for both PET (tracer quantities 10^{-9} to 10^{-12} M) and MRI (tracer quantities 10^{-4} M) imaging applications.

To sum up…

Although radiolabeled NPs have shown great promise in SPECT/PET imaging of diseases, several challenges need to be addressed to translate the radiolabeled NPs to clinical applications:

- Development of truly tissue–selective targeting NPs without the significant uptake in the mononuclear phagocytic system (MPS) To resolve this issue, the NPs can be designed with optimal surface modifications
- Functionalization of NPs with antibodies, peptides or other targeting ligands that recognize specific receptors or antigens have the potential to increase the target-to-background ratio
- Design considerations (shape, charge, size, surface coating, and dosing) can be manipulated to prolong blood circulation, reduce the nonspecific distribution, and enhance imaging contrast.
- In order to achieve optimal target–to–background contrast in SPECT/PET, good *in vivo* stability of radiolabeled NPs is also required

In conclusion, radiolabeled NPs have shown great promise in SPECT/PET imaging. With the development of hybrid imaging technology, we expect that novel radiolabeled NPs with SPECT/PET along with other imaging modalities will afford accurate and precise assessment of biological signatures in a real–time manner and thus improve disease management.

The design of the appropriate multi-modal imaging probe is vital and any real advances in molecular imaging will be due to the ***interdisciplinary efforts*** of synthetic chemists, molecular biologists, imaging scientists and clinicians.

Acknowledgments

•Dr. Charalampos Tsoukalas, INRaSTES, NCSR “Demokritos”
•Dr. T. Tsotakos, INRaSTES, NCSR “Demokritos”
•Dr. Demosthenis Stamopoulos, INN, NCSR “Demokritos”
•Dr. Maria Paravatou-Petsotas, INRaSTES, NCSR “Demokritos”

•Dr. Constantinos Anagnostopoulos, Center for Experimental Surgery, Clinical and Translational Research, Biomedical Research Foundation, Academy of Athens
•Dr. Anastasios Gaitanis, Center for Experimental Surgery, Clinical and Translational Research, Biomedical Research Foundation, Academy of Athens
•Dr. George Kastis, Research Center of Mathematics, Academy of Athens

•Dr. Angela Moulopoulos, Aretaieion University Hospital
•Dr. Vasileios Koutoulidis, Aretaieion University Hospital

•Professor Olivier Tillement, Universite Claude Bernard Lyon 1, Laboratoire de Physico-Chimie des Materiaux Luminescents - Lyon, France
•Professor Francois Lux, Universite Claude Bernard Lyon 1, Laboratoire de Physico-Chimie des Materiaux Luminescents - Lyon, France

•Professor Stephane Roux, Université de Franche-Comté, Institut UTINAM, UMR 6213 CNRS-UFC,Besançon Cedex, France

•Professor Dr. Frank Roesch, Institute of Nuclear Medicine, Johannes Gutenberg University, Mainz, Germany
•Professor Dr. Helmut R. Maecke, Department für Radiologische Diagnostik und Therapie Klinik für Nuklearmedizin, University Hospital Freiburg, Freiburg, Germany

cost
EUROPEAN COOPERATION IN SCIENCE AND TECHNOLOGY

COST TD1004: “Theranostics Imaging and Therapy: An Action to Develop Novel Nanosized Systems for Imaging-Guided Drug Delivery”

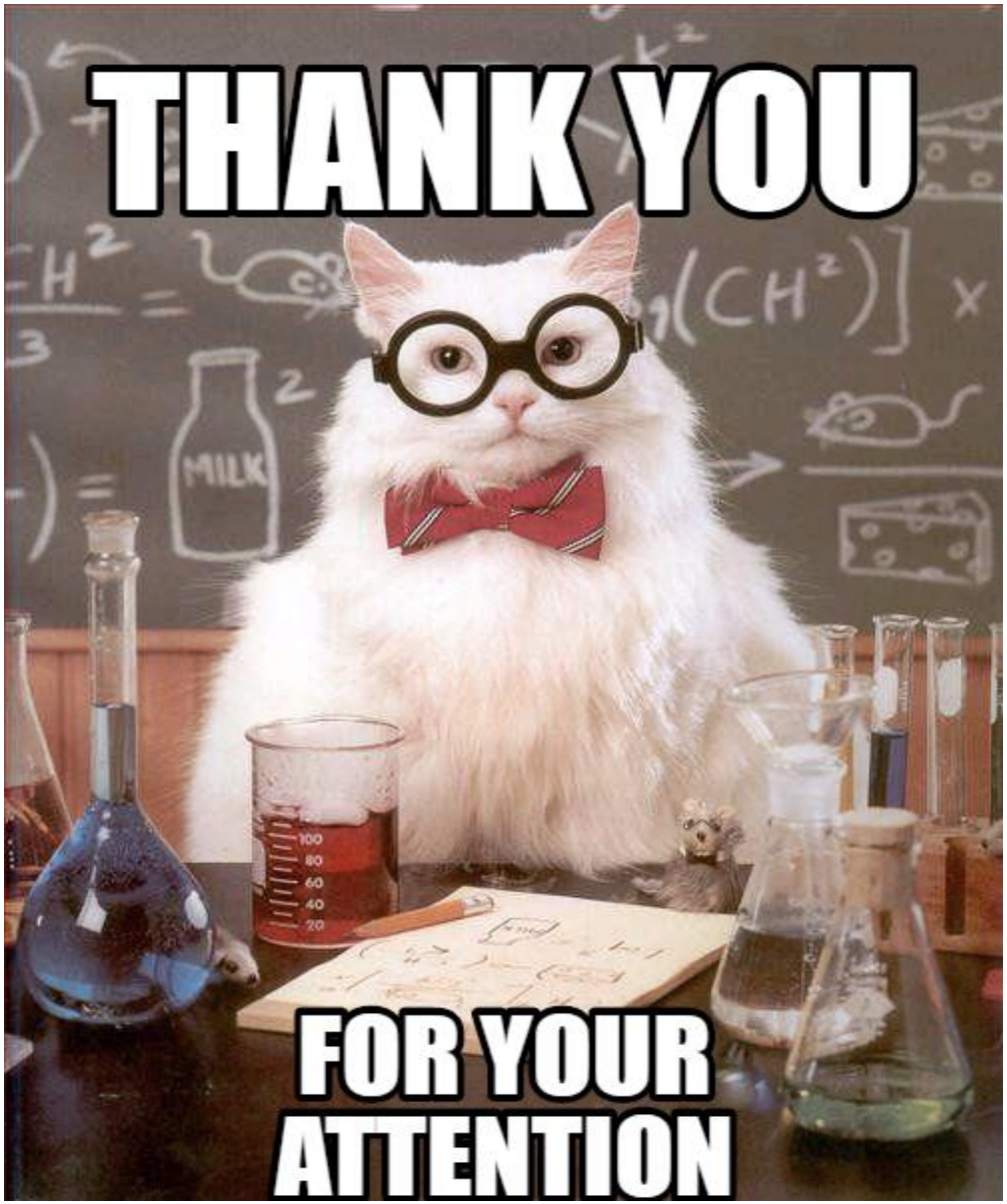
THANK YOU
MILK
FOR YOUR
ATTENTION